

Comparison of the H₂O₂ density distribution in the effluent of a COST-Jet and kINPen measured with cavity ring-down spectroscopy

B. Harris¹, L. Krös², A. Nave², E. Wagenaars¹, and J. H. van Helden²

¹ York Plasma Institute, School of Physics, Engineering and Technology, University of York, York, United Kingdom

² Leibniz Institute for Plasma Science and Technology (INP), Greifswald, Germany

Abstract: In this study, the density distribution of H₂O₂ in the effluent of a COST-Jet and kINPen is characterised with the use of cavity ring-down spectroscopy. The ν_6 absorption band of H₂O₂ is probed to obtain its line-of-sight integrated density. The distribution of this parameter is found to be Gaussian along the radius of the effluent, allowing an Abel inversion to be performed to determine spatially resolved H₂O₂ densities within the full effluent region. A comparison is then drawn between the two sources investigated.

Keywords: Cavity ring-down spectroscopy, cold atmospheric-pressure plasmas

1. Introduction

Cold atmospheric-pressure plasma jets (CAPJs) supplied with helium and water vapour are ideal sources of reactive oxygen species for biomedical applications. H₂O₂ can be produced by these plasmas in appreciable quantities and plays an important role in plasma-assisted wound healing and microbial sterilisation [1]. Previous studies have investigated the presence of H₂O₂ in the plasma afterglow, plasma-treated liquids, and biological media [2-4]. However, this study marks the first experimental work in which the density of H₂O₂ is fully spatially resolved in the gas phase of CAPJs supplied with a helium feed gas. Two CAPJs are investigated in this work. The first is the COST Reference Microplasma Jet (or COST-Jet). The COST-Jet is a parallel-plate, capacitively coupled plasma source designed to act as a reference standard that has also seen use in applied research [5,6]. The second CAPJ is the kINPen, a CE-certified and commercially available plasma jet consisting of a pin-type powered electrode within a dielectric capillary [7]. The differing electrode geometries and power regimes between the two sources result in differing effluent H₂O₂ distributions, which may influence which CAPJ is better suited for a given application. It is for this reason that this study draws a comparison between the two.

2. Experimental Setup

A helium feed gas is used at a flow rate of 1 SLM. The helium is humidified by guiding 0.2 SLM of it through a bubbler, such that the CAPJs are also supplied with 3200 ppm of water vapour. A schematic of the CAPJs is shown in Fig. 1. The position in the effluent is normalised to the nozzle of the jet in question, with the centre of the nozzle having transverse (x) and axial (z) positions of 0 mm.

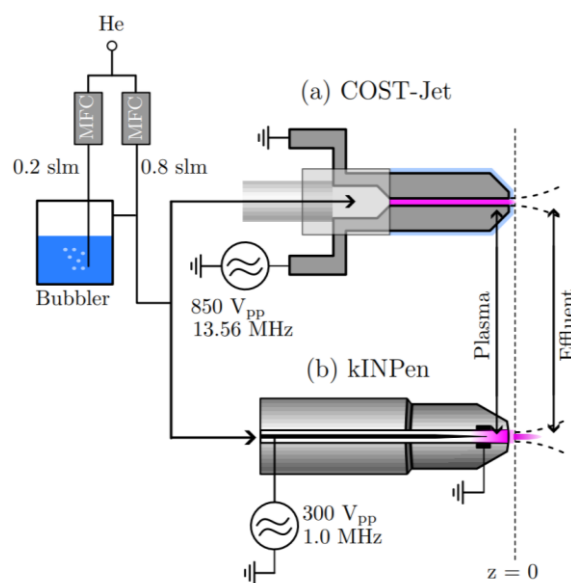


Fig. 1. The CAPJs investigated in this work. Both are supplied with 1 SLM He + 3200 ppm H₂O.

Experimental measurements are performed using continuous wave cavity ring-down spectroscopy. The effluent region is analysed by mounting a CAPJ within an optical cavity, consisting of two highly reflective mirrors. A mid-infrared (8 μ m) quantum cascade laser is coupled into the cavity. When a given threshold intensity is reached, the laser is switched off. The time taken for this signal to decay, known as the ring-down time, is dependent on absorption from species distributed along the optical path length. Using this relationship, the line-of-sight integrated density of H₂O₂ is extracted from a chosen absorption feature in the ν_6 band of H₂O₂ by applying a model fit using parameters provided by the HITRAN database [8,9]. An example of the measured absorption feature and applied fit is shown in Fig. 2.

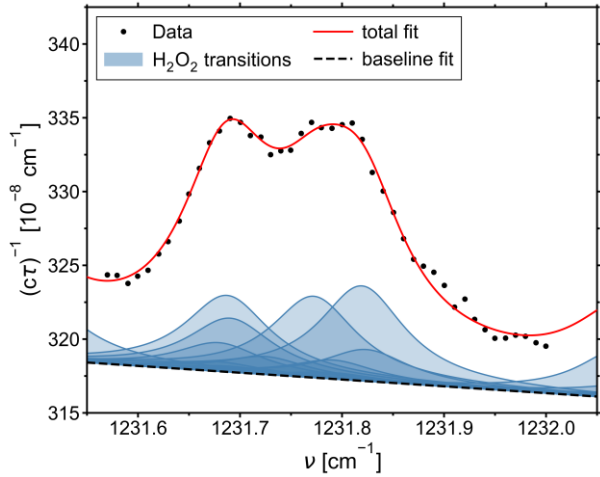


Fig. 2. Model fit to H_2O_2 absorption feature. $(c\tau)^{-1}$ is proportional to the total absorption along the optical cavity, where τ is the ring-down time and c is the speed of light in a vacuum.

3. Results and Discussion

Line-of-sight integrated H_2O_2 densities, n_{int} are recorded across the radius of the effluent. These transverse distributions were found to be well approximated by a Gaussian shape, with an error-weighted fit being applied to extract each distribution's width, w and peak H_2O_2 density, n_0 using the following:

$$n_{int}(x) = \sqrt{\frac{\pi}{2}} w n_0 \exp\left(-2 \frac{x^2}{w^2}\right) \quad (1)$$

An example of this fit is shown in Fig. 3. Eq. (1) is arranged such that an Abel inversion can be performed using the extracted parameters:

$$n(x, y) = n_0 \exp\left(-2 \frac{x^2 + y^2}{w^2}\right) \quad (2)$$

where $n(x, y)$ represents the spatially resolved density of H_2O_2 on the plane perpendicular to the plasma jet.

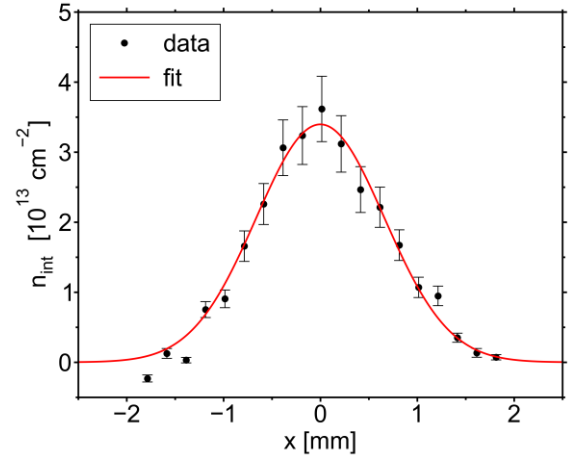


Fig. 3. Gaussian fit to line-integrated densities of H_2O_2 , distributed transversally across the plasma effluent.

The distribution of H_2O_2 along the axis of the effluent is characterised by extracting the width and peak H_2O_2 density at several axial positions. The resulting profiles can be described with polynomial functions. Thus, substituting these functions into Eq. (2) allows the density of H_2O_2 to be calculated for any given position in the effluent of the COST-Jet and kINPen. The results of this are shown in Fig. 4, with the black bars representing regions outside the range of measurement. The H_2O_2 densities measured for the kINPen are a factor of roughly 2 higher than those for the COST-Jet, though it must be stressed that it is not possible to decipher whether this is a result of the jet design or of the power supplied to the devices. It is known that the density of H_2O_2 is clearly correlated with the power deposited into the plasma. However, it was not possible to experimentally match the power deposition of both CAPJs and so a comparison of absolute densities should be

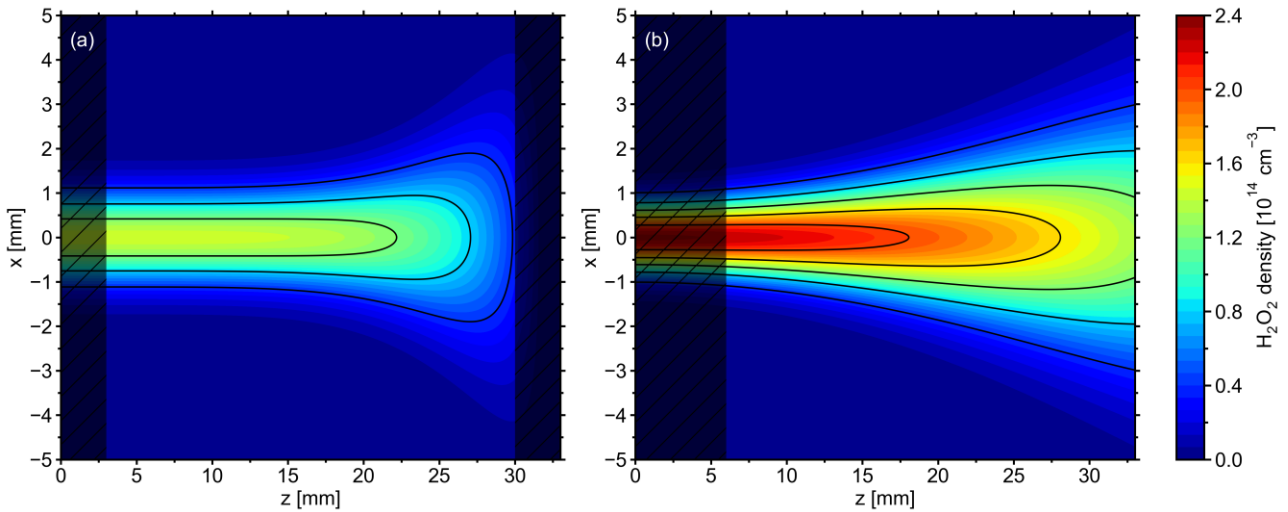


Fig. 4. H_2O_2 density distributions in the effluent of (a) a COST-Jet and (b) a kINPen.

avoided. The focus of this analysis is therefore on comparing the distribution of H_2O_2 throughout the effluent. It is observed that the H_2O_2 flow profile of the COST-Jet is initially highly laminar, with little change in the Gaussian width or peak density observed below $z = 20$ mm. There is a sharp decline past this point, where the flow degrades and the H_2O_2 disperses more widely into the open air. In the case of the kINPen, the initial profile is appreciably less laminar, however it is seen to be more consistent further into the effluent and does not experience the same sharp drop in density as the COST-Jet. The axial density gradient of both CAPJs also suggest that the bulk of H_2O_2 formation occurs within, or a few millimetres after, the plasma channel rather than further into the effluent.

4. Conclusion

The distribution of H_2O_2 in the effluent of two cold atmospheric-pressure plasma jets, the COST-Jet and kINPen, have been investigated using continuous wave cavity ring-down spectroscopy. Line-of-sight integrated densities of H_2O_2 were obtained from measurements of an absorption feature in the ν_6 band of H_2O_2 for both plasma jets. The distribution of these line-integrated densities was found to be well-approximated by a Gaussian in the transverse direction. Extracting parameters from the Gaussian fit in turn allowed the behaviour of the distribution along the axis of the effluent to be characterised with polynomial functions. Combining the Gaussian and polynomial functions and performing an Abel inversion on the result produced spatially resolved densities of H_2O_2 within the effluent region. This result was then compared between the two plasma jets investigated.

5. Acknowledgements

The authors would like to thank Sarah-Johanna Klose for developing the cavity setup utilised in this study. This work was partly funded by INP internal funding. We also acknowledge financial support from the UK EPSRC (EP/K018388/1 & EP/H003797/2) and the Norma Ann Christie Scholarship.

6. References

- [1] S.K. Dubey, et al. *Process Biochemistry*, 112 (2022).
- [2] J. Winter, et al. *Journal of Physics D: Applied Physics*, 47(28) (2014).
- [3] J. Winter, et al. *Journal of Physics D: Applied Physics*, 46(29) (2013).
- [4] Y.F. Yue, et al. *IEEE Transactions on Plasma Science*, 44(11) (2016).
- [5] J. Golda, et al. *Journal of Physics D: Applied Physics*, 49(8) (2016).
- [6] Y. Gorbanev, et al. *Plasma*, 2(3) (2019).
- [7] S. Reuter, et al. *Journal of Physics D: Applied Physics*, 51(23) (2018).
- [8] S. Klee, et al. *Journal of molecular spectroscopy*, 195(1) (1999).
- [9] I.E. Gordon, et al. *Journal of quantitative spectroscopy and radiative transfer*, 277 (2022).